Journal of Biosciences and Medicines, 2026, 14(4), 128-141
https://www.scirp.org/journal/jbm
ISSN Online: 2327-509X
ISSN Print: 2327-5081

Network-Based Structural Analysis of SARS-CoV-2 Spike Variants Using Protein Structure Networks

Michelle Fuentes-Acosta[1,2], Jorge Mulia-Rodríguez[1], Daniel Osorio-González[1*]

[1]Molecular Biophysics Laboratory, Faculty of Sciences, The Autonomous University of the State of Mexico, Toluca, Mexico
[2]Center for Research, Technology Transfer, and Business Innovation, Metepec, Mexico
Email: *dog@uaemex.mx

How to cite this paper: Fuentes-Acosta, M., Mulia-Rodríguez, J. and Osorio-González, D. (2026) Network-Based Structural Analysis of SARS-CoV-2 Spike Variants Using Protein Structure Networks. *Journal of Biosciences and Medicines*, **14**, 128-141.
https://doi.org/10.4236/jbm.2026.144011

Received: March 5, 2026
Accepted: April 12, 2026
Published: April 15, 2026

Abstract

Severe acute respiratory syndrome coronavirus 2 (SARS-CoV-2) is a zoonotic virus responsible for the respiratory disease COVID-19. The rapid spread of the virus has led to the emergence of variants containing mutations that modify viral dynamics, increase transmissibility, and affect vaccine effectiveness. Among the structural proteins of SARS-CoV-2, the Spike glycoprotein plays a fundamental role in the infection process because it mediates recognition and binding to the human angiotensin-converting enzyme 2 (ACE2) receptor. In this work, structural and topological properties of Spike protein variants Alpha (B.1.1.7), Beta (B.1.351), Delta (B.1.617), and Omicron 23A (XBB.1.5) were analyzed using a protein structure network (PSN) framework. Three-dimensional structural models were generated from experimental templates, and residue interaction networks were constructed using alpha-carbon atoms as nodes and a distance threshold of 7 Å. Graph-theoretical metrics—including degree, betweenness, closeness, clustering coefficient, eigenvector centrality, and eccentricity—were calculated to identify key insights involved in structural communication pathways. Preliminary analysis indicates that mutations associated with major variants alter network topology and may affect long-range communication between structural domains of the Spike protein. These findings provide a computational framework for detecting mutation-sensitive regions and potential targets for antiviral intervention.

Keywords

SARS-CoV-2, Spike Protein, Protein Structure Networks, Structural Bioinformatics, Graph Theory, Viral Variants

1. Introduction

SARS-CoV-2 emerged in late 2019 and rapidly spread worldwide, leading to the COVID-19 pandemic [1]-[4]. The virus belongs to the β-coronavirus family and is responsible for a respiratory disease that has caused significant global health, economic, and social impacts [4] [5]. A key factor contributing to the persistence and evolution of SARS-CoV-2 is the emergence of variants containing mutations that modify viral transmissibility, immune escape capacity, and receptor-binding affinity [6].

The Spike glycoprotein is the primary mediator of viral entry into host cells because it recognizes and binds to the ACE2 receptor located on human cells [7]-[9]. Structurally, the Spike protein is divided into two subunits, S1 and S2. The S1 subunit contains the receptor-binding domain (RBD), responsible for host receptor recognition, while the S2 subunit mediates membrane fusion. Crucially, the Spike protein is a highly dynamic molecular machine that undergoes significant conformational rearrangements. The RBDs exist in an equilibrium between a "closed" (down) state, which hides the receptor-binding site to evade immune detection, and an "open" (up) state, which is required to engage the ACE2 receptor [7] [8]. Mutations in the Spike protein can alter its structural dynamics and therefore influence viral infectivity and immune recognition [10].

Recent advances in computational biology have enabled the study of protein structures using network-based approaches. Protein structure networks represent amino acids as nodes connected through interactions derived from spatial proximity or interaction energy [11]. This representation allows the application of graph theory to identify residues involved in structural communication, energy transfer, and allosteric regulation [12].

In this study, we analyze the structural organization of the Spike protein from several major SARS-CoV-2 variants using a network-based framework. By combining structural modeling and graph-theoretical analysis, we first characterize the topological transition between the closed and open conformational states of the Spike protein. Subsequently, we compare major variants within the closed state to identify differences that may play important roles in structural stability and communication within the Spike protein.

2. Materials and Methods

2.1. Variant Selection

The variants of Concern (VOCs) Alpha (B.1.1.7), Beta (B.1.351), Delta (B.1.617), and Omicron 23A (XBB.1.5) were selected based on their global epidemiological impact and prevalence between January 2021 and January 2023 as identified by Nextstrain phylogenetic analysis (**Figure 1**) [13] [14].

2.2. Sequence Identification

Consensus amino-acid sequences of the Spike protein for each variant were re-

trieved from covSPECTRUM platform which aggregates genomic surveillance data from the GISAID database [15] [16]. The selection of the sequences was based on "Consensus sequence" feature, which identifies the most frequent amino acid mutations at each position for a specific variant.

Each retrieved sequence was validated through a BLAST alignment against the reference sequence of SARS-CoV-2 Spike protein (NCBI ID: YP_009724390.1) to confirm the presence of lineage-defining mutations. Furthermore, sequences were cross-referenced with the GISAID (**Figure 2**) to ensure they accurately represented the international consensus for each Variant of Concern (VOC) at the time of the study.

2.3. Structural Modeling

Three-dimensional structural models were generated using an experimentally determined Spike structure (PDB ID: 7JJI) as the primary template. This template was selected because it represents a full-length (FL) prefusion spike trimer including the transmembrane (TM) domain and cytoplasmic tail (CT), providing a more biologically relevant framework of the closed state (3-RBD-down) of Spike [17]. The experimentally based template was pre-processed by computationally removing all non-amino acid moieties to eliminate potential stereochemical interference. Missing residues—of wild type (WT) and VOCs structures—were reconstructed using homology modeling tools with the SWISS-MODEL pipeline.

In parallel, a fully computational model was developed to be used as a comparative template for assessing the impact of conformational changes of Spike protein. Unlike the experimental template, this *in silico* model has one RBD in the "up" (open) conformation, representing the state primed for interaction with the ACE2 receptor. For WT, both experimental-based and computationally-model structures were generated in order to compare structural changes due to conformational rearrangement.

The comparative analysis between variants was conducted exclusively using the networks derived from the experimental-based template, due to its superior structural quality and stability.

The structural reliability of these models was further validated through complex network analysis, following the criteria of Pražnikar *et al.* (2019), which distinguishes correct structural models based on global topological signatures [18]. For this purpose, protein structure networks were constructed following the parameters described in the next section.

2.4. Protein Structure Network Construction

Protein structure networks were constructed for the spike trimer assemblies using alpha-carbon (Cα) atoms as nodes. Edges between nodes were defined based on a distance threshold of 7 Å between Cα atoms. This distance threshold was applied indiscriminately to both intra-chain and inter-chain contacts, allowing for the capture of critical communication pathways across the protein.

The use of Cα nodes and a 7 Å cutoff is a well-established approach for identifying legitimate residue contacts while minimizing noise from side-chain fluctuations. A 7 Å threshold represents a "topological signature" of the first coordination shell in proteins. This ensures that the network captures all complete and non-occluded contacts, providing a reliable basis for interpreting centrality and information flow within the large-scale Spike trimer [19].

To ensure a statistically consistent comparison of network metrics between the "open" and "closed" states of WT Spike, the node sets were equalized across both structural scaffolds. The computational model was processed to match the sequence coverage of the experimental template for the final network construction.

Network analysis was performed using Python-based computational tools implemented within the Anaconda data science environment, while visual representations were made with Cytoscape [20].

2.5. Network Metrics

The following graph-theoretical metrics were calculated: node degree, betweenness centrality, closeness centrality, clustering coefficient, eigenvector centrality, and eccentricity [21] [22]. These measures allow the identification of residues involved in communication pathways and structural connectivity within the protein.

To establish a baseline for the protein's mechanics, a comparative analysis was first performed between the "open" and "closed" states using the reference sequence (Wild-Type) structure for both the experimental-based template (3-RBD-down) and the computational-based template (1-RBD-up). This approach ensures that the fundamental topological shifts associated with the RBD transition are captured.

Subsequently, the analysis of SARS-CoV-2 of VOCs was conducted exclusively using networks derived from the experimentally based template. This strategy was chosen to maintain high structural fidelity across the comparative framework.

Statistical analyses were performed to evaluate topological differences across conformational states and viral variants. To determine the statistical significance of changes between the "open" (1-RBD-up) and "closed" (3-RBD-down) states, the non-parametric Mann-Whitney U test was employed, while for the comparative analysis among VOCs, a Welch's ANOVA was conducted followed by post-hoc tests.

3. Results

3.1. Variant Sequence Analysis

Analysis of genomic surveillance data revealed that the variants Alpha, Beta, Delta, and Omicron represented major waves of global SARS-CoV-2 transmission [23]. The temporal prevalence of these variants and their global distribution during the pandemic are illustrated in **Figure 1**.

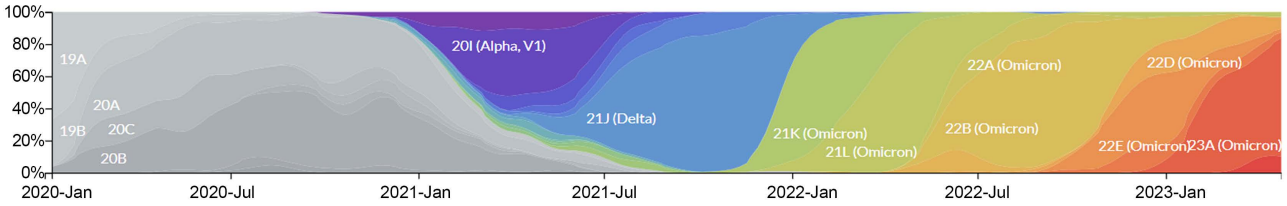

Figure 1. Global prevalence of major SARS-CoV-2 variants during the COVID-19 pandemic**.** The figure illustrates the frequency of reported COVID-19 cases associated with the Alpha (B.1.1.7), Beta (B.1.351), Delta (B.1.617), and Omicron (XBB.1.5) variants over time. Data were obtained from global genomic surveillance platforms and represent the relative prevalence of each variant during different phases of the pandemic. Graph obtained from the Nextstrain [23].

Each variant contained characteristic mutations within the Spike protein sequence, particularly within the receptor-binding domain and the N-terminal domain. These mutations are known to influence receptor binding affinity, antibody recognition, and viral infectivity. The distribution and prevalence of mutations across the Spike protein sequence for each variant are shown in **Figure 2**.

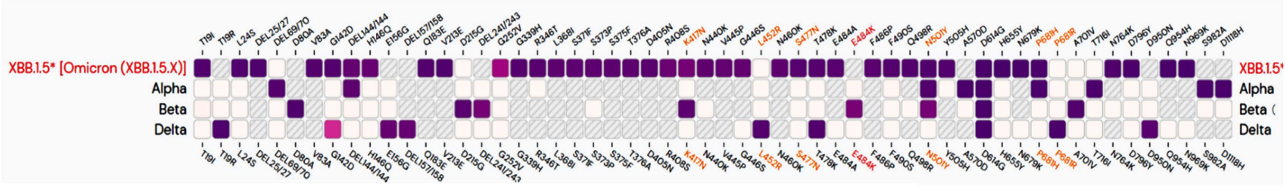

Figure 2. Distribution and prevalence of mutations in the SARS-CoV-2 Spike protein across major variants. Heatmap representation of mutation frequencies within the Spike protein sequence for the Alpha, Beta, Delta, and Omicron variants. Darker colors indicate higher mutation prevalence at specific amino-acid positions. Data were compiled from the GISAID database [15].

3.2. Structural Model Generation

Three-dimensional structural models were successfully generated for the Spike protein trimer of WT and each variant. Structures derived from experimental templates included residues from positions 14 to 1146, whereas the original computational model incorporated the full sequence length (1 - 1273) and was subsequently processed to match the experimental template coverage. Representative structural models of the Spike protein for the Alpha, Beta, Delta, and Omicron variants, highlighting the mutations, are shown in **Figure 3**.

Models derived from the experimental template achieved an average QMEANDisCo score of 0.74 ± 0.05 and GMQE of 0.67, while these scores reflect some local uncertainty in highly flexible loops—inherent to the dynamic nature of the Spike protein and the limitations of experimental recovery in those regions—they indicate a high degree of structural reliability for the folded domains. In parallel, the fully computational model yielded a lower average QMEANDisCo score of 0.62 ± 0.05 and GMQE of 0.67. The slightly superior performance is likely attributed to the "closed" (3-RBD-down) conformation of the 7JJI template, since by maintaining all three RBDs in the down position, the structure achieves a more compact arrangement, which might reduce the conformational uncertainty of the protein's flexible regions—particularly RBDs—by limiting their range of motion, compared

to the open state. However, in terms of stability, recent studies demonstrate that SARS-CoV-2 variants have developed an "open spike" strategy, characterized by greater kinetic stability of the open conformation to facilitate interaction with the ACE2 receptor [25].

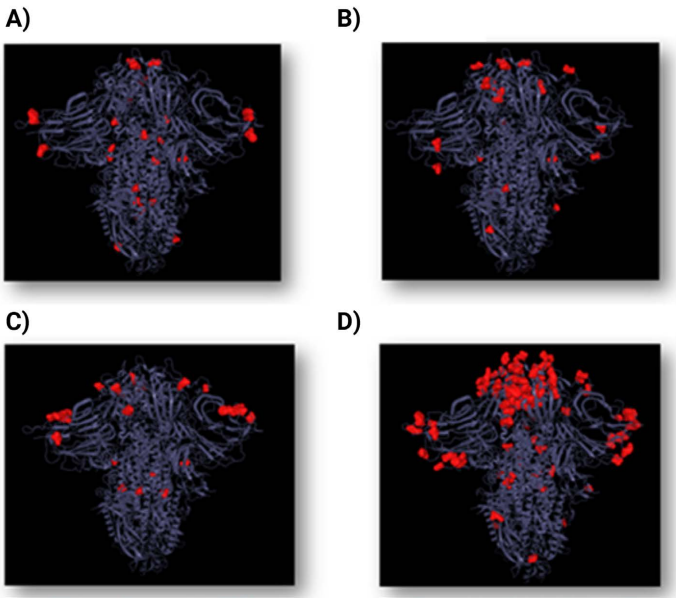

Figure 3. Three-dimensional structural models of SARS-CoV-2 Spike variants. Structural representations of the Spike protein trimers for the Alpha (A), Beta (B), Delta (C), and Omicron (D) variants. These models highlight the differences arising primarily from variant-specific mutations affecting the RBD and surrounding regions. Images obtained from ViralZone [24].

This divergence justifies our strategy of utilizing the experimentally based networks as the primary framework for variant comparison, as it provides a better topological scaffold for detecting mutation-induced changes without the added complexity of "up" state conformation.

3.3. Network Topology Analysis

Protein structure networks were generated for each conformational state to characterize the underlying residue interaction patterns. Visual representation of the trimer alignment (**Figure 4(A)**) and the resulting networks for the closed (**Figure 4(B)**) and open (**Figure 4(C)**) states reveals that while the global scaffold remains, the mechanical activation of the receptor-binding domain (RBD) induces a localized topological reconfiguration.

Networks generated for each variant displayed similar global connectivity patterns but showed local differences associated with mutation sites. The comparison of the protein structure network representation of the Spike protein VOCs is shown in **Figure 5**. The average node degree values fell within the expected range for correctly folded protein structures [18]. This indicates that the generated structural models maintain realistic residue interaction patterns.

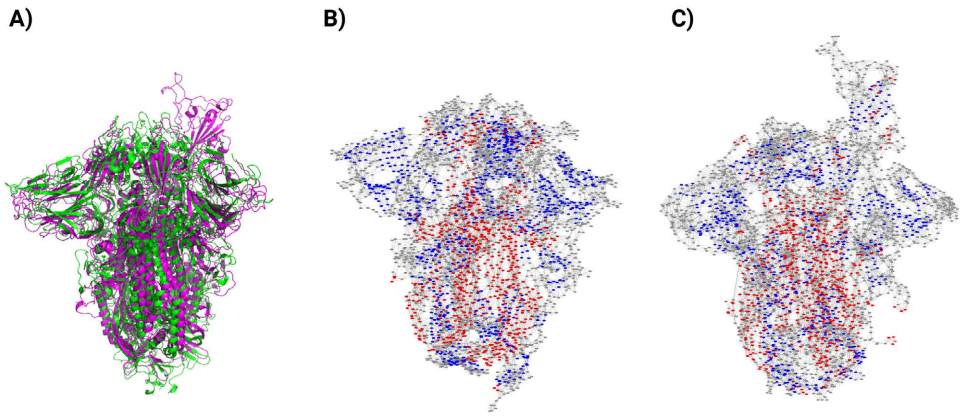

Figure 4. Conformational and network representation of the SARS-CoV-2 Spike protein. (A) Structural alignment between the closed (all-RBD-down in green) and open (one-RBD-up in magenta) states. (B) Residue interaction network of the trimer in the closed state. (C) Residue interaction network in the open state. Nodes are colored by secondary structure, in red α-helices, in blue β-sheets and in grey loops.

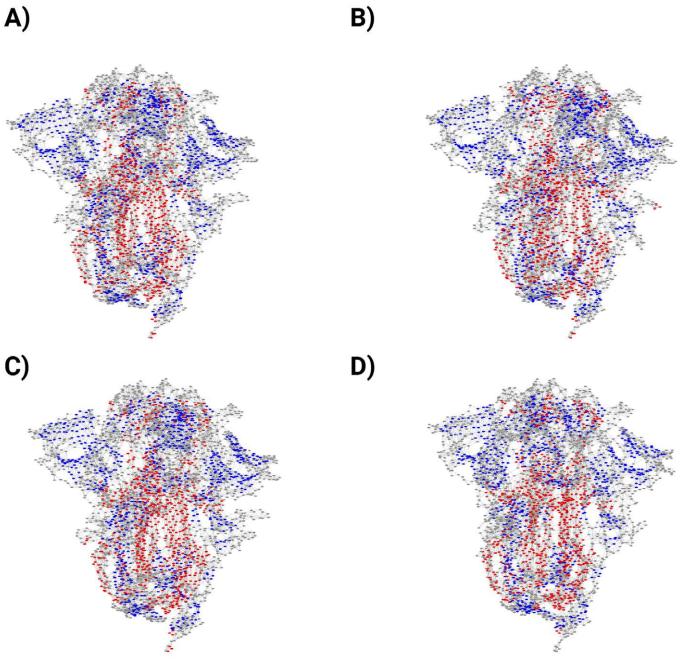

Figure 5. Comparative protein structure networks across SARS-CoV-2 Variants of Concern (VOCs). Visual representation of the residue interaction networks in the closed state for (A) Alpha, (B) Beta, (C) Delta, and (D) Omicron variants. Nodes are colored by secondary structure: red (α-helices), blue (β-sheets), and grey (loops).

3.4. Centrality Analysis of Open and Closed Conformational States

The structural changes Spike overcomes to shift from the closed (all-RBD-down) to the open (one-RBD-up) state induced a significant global rearrangement of the protein's network topology. Statistical comparisons of centrality measures demonstrated that while the distributions of closeness centrality ($p < 0.001$), eigenvector centrality ($p < 0.001$), degree ($p = 0.050$), and eccentricity ($p < 0.001$) shifted sig-

nificantly, the global communication of the backbone remained, as evidenced by the non-significant variations in betweenness centrality ($p = 0.337$) and the clustering coefficient ($p = 0.070$). Nevertheless, visual analysis of the centrality profiles reveals that despite the statistical stability of the overall betweenness distribution, there is a clear reorganization of communication pathways across the trimer; specifically, chain C exhibits a marked increase in betweenness peaks (**Figure 6(A)**) when its RBD is in the "up" position, suggesting a localized concentration of information flow. This is accompanied by a localized increase in eigenvector centrality (**Figure 6(B)**) and a marked change in eccentricity (**Figure 6(C)**), reflecting a redistribution of node influence and structural distance within the activated protomer which can also be observed in the distinct reduction in closeness centrality values within the Chain C RBD during activation, as the structural opening increases the shortest path distances between the protruding domain and the rest of the protein network (**Figure 6(D)**). The significant differences in degree distributions reflect a localized gain in connectivity for specific residues during the RBD extension (**Figure 6(F)**), whereas the stability of the clustering coefficient indicates that the local modularity and the density of neighboring interactions remain largely unaffected by the conformational change (**Figure 6(E)**). These hierarchical modifications indicate a transition toward a functionally primed state, consistent with the increased kinetic stability of open spike conformations observed by Yang and collaborators (2022).

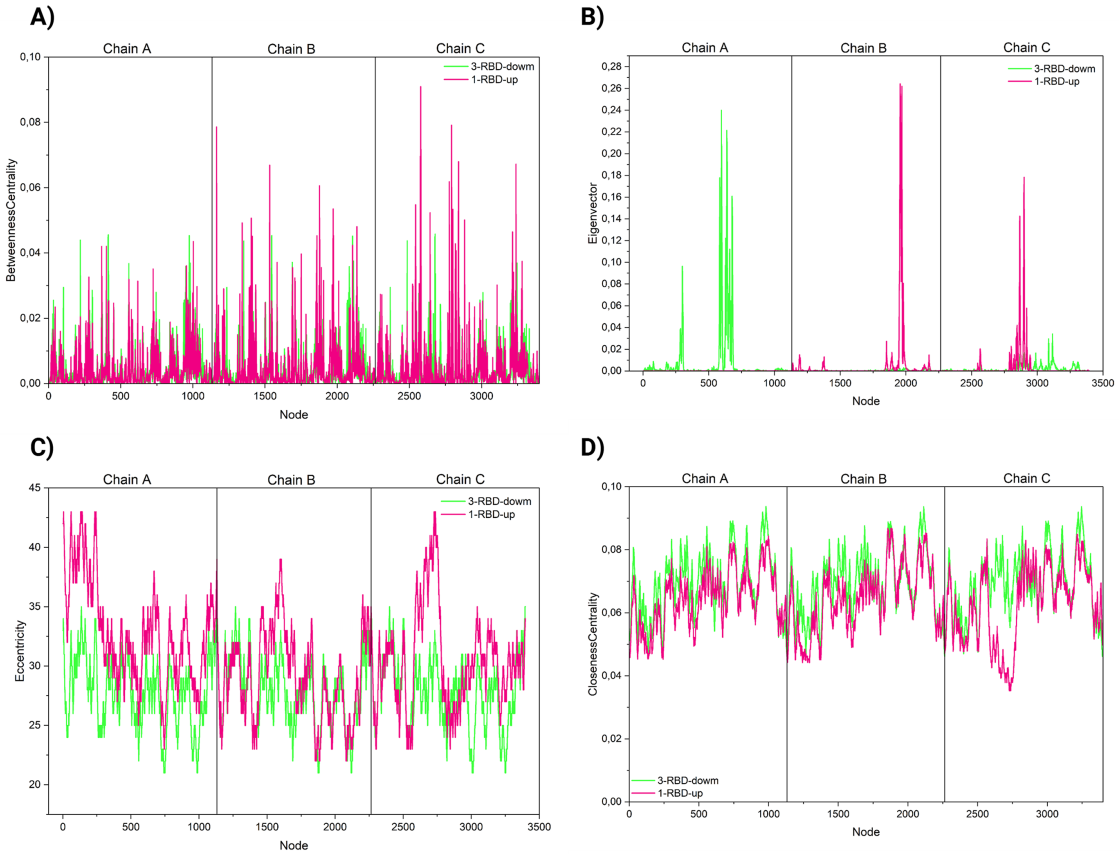

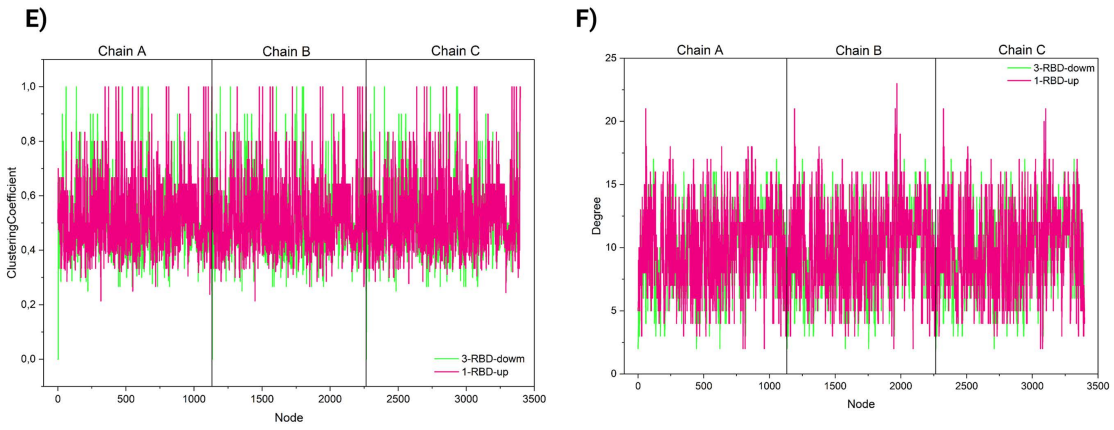

Figure 6. Comparative analysis of network centrality metrics between the closed and open states of the SARS-CoV-2 Spike protein. The topological profiles for the Wild-Type reference sequence are shown for the "closed" (3-RBD-down, green line) and "open" (1-RBD-up, magenta line) conformations. The metrics include (A) Betweenness Centrality, (B) Eigenvector Centrality, (C) Eccentricity, (D) Closeness Centrality, (E) Clustering Coefficient, and (F) Degree.

3.5. Centrality Analysis of Spike Variants

The comparative analysis among VOCs within "closed" state, revealed that lineage-specific mutations induce a targeted reorganization of the protein's hierarchical influence rather than a global structural breakdown. There were no significant differences in the distributions of betweenness centrality, closeness centrality, degree, and clustering coefficient across variants ($p > 0.05$), indicating a high degree of conservation in the trimer's fundamental backbone (**Figure 7**). However, significant statistical divergence was identified in eigenvector centrality (EC) and eccentricity ($p< 0.001$), suggesting that mutations in Alpha, Beta, Delta, and Omicron variants strategically reconfigure node influence and structural distances. Post-hoc tests confirmed that Omicron was the most divergent lineage, showing significant differences in eigenvector centrality compared to all other variants ($p < 0.001$).

The nodes with the highest eigenvector centrality are those connected to other highly central nodes, making this metric a robust way of determining a node's dominance and its role as a principal channel for information flow within the network [26] [27]. Furthermore, changes in eccentricity between the VOCs ($p = 0.011$) shows a redistribution of the protein's structural distances, since—an amino acid with high eccentricity in comparison to the network's average—will be impacted more rapidly by other residues or, conversely, may easily affect numerous amino acids, suggesting that mutational shifts in both of this metrics optimize the speed and reach of allosteric signaling [26].

It is noticeable that while Alpha and Delta variants concentrate their primary values of EC in chain C and A, respectively, Omicron exhibits distributed EC values across the entire trimer. This transition from centralized to distributed dominance hubs may reflect an evolutionary trend towards a more resilient allosteric network. The topological characteristic of the Omicron variant identified in this

study is strongly supported by recent Protein Contact Network (PCN) analyses, which similarly highlight Eigenvector Centrality as a distinctive topological feature of Omicron, contrasting with Alpha and Delta. Apparently, this shift is independent of the total number of mutations, representing instead a qualitative change in the role of mutated residues within the network [28].

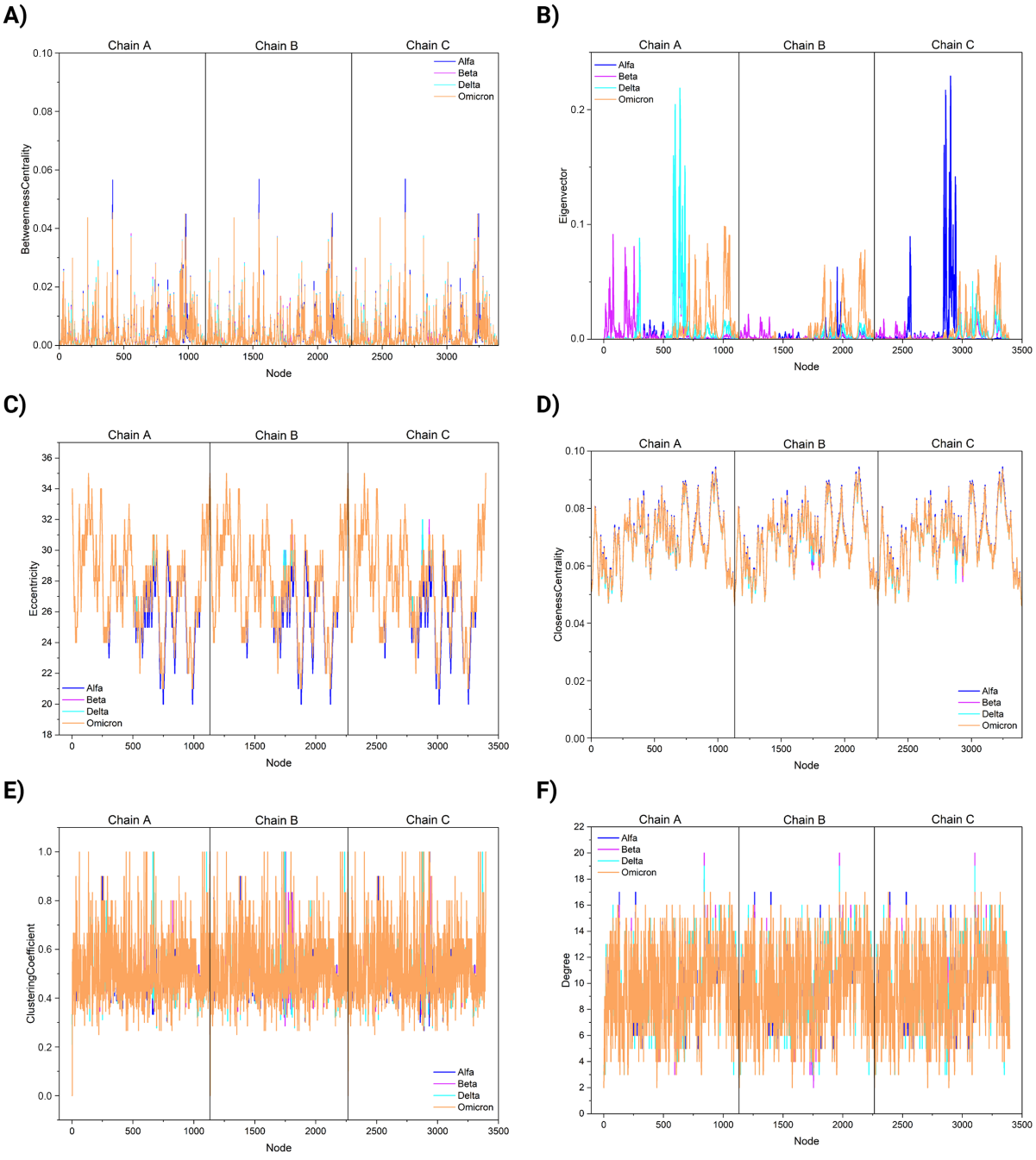

Figure 7. Comparative network centrality profiles across SARS-CoV-2 Variants of Concern (VOCs). Topological distributions are shown for Alpha (dark blue), Beta (magenta), Delta (cyan), and Omicron (orange) variants in the closed state. The panels display (A) Betweenness Centrality, (B) Eigenvector Centrality, (C) Eccentricity, (D) Closeness Centrality, (E) Clustering Coefficient, and (F) Degree.

Centrality analysis also revealed that residues located within the receptor-binding domain and the subunit interface exhibited high betweenness centrality values (**Figure 7(A)**). These residues likely act as communication hubs within the protein structure. Mutations present in certain variants were found near residues with high centrality values, suggesting that these mutations may alter structural communication pathways and influence long-range interactions within the protein.

Comparative analysis between variants suggests that mutations associated with highly transmissible variants may affect network connectivity between structural domains of the Spike protein. In particular, changes near the receptor-binding motif may influence communication between the S1 and S2 subunits, potentially altering conformational dynamics involved in viral entry [29]-[32].

4. Conclusions

This study presents a network-based structural framework for analyzing the Spike protein of SARS-CoV-2 conformational changes due to RBD opening or induced by mutation of VOCs. The integration of protein structure networks and graph-theoretical metrics enables the identification of residues involved in structural communication and potential mutation-sensitive regions.

The results suggest that mutations in major variants may influence the topology of residue interaction networks and alter communication pathways within the protein. These changes may contribute to differences in viral transmissibility and immune escape. Although this approach provides a foundation for identifying key structural nodes, findings are bounded by certain limitations, such as the use of static structural models which do not account for intrinsic protein dynamics, and the analysis of the apo-form that excludes the influence of the glycan shield on stability and immune recognition. Furthermore, homology modeling provided a complete scaffold, however, the structural reliability of rebuilt flexible regions remains subject to the uncertainties of computational prediction.

While the static network analysis provides a robust baseline of the trimer's topological integrity, the observed shifts in eigenvector centrality associated with the VOCs likely represent the structural priming required for the protein's dynamic transitions.

Future work will focus on integrating dynamic simulation of VOCs and machine learning models to predict mutation-sensitive regions and to identify potential therapeutic targets within the Spike protein.

Conflicts of Interest

The authors declare no conflicts of interest regarding the publication of this paper.

References

[1] World Health Organization (2020) Coronavirus Disease (COVID-2019) Situation Reports. World Health Organization.

[2] Worldometer (2022) COVID-19 Coronavirus Pandemic.

https://www.worldometers.info/coronavirus/

[3] World Health Organization (2023) Statement on the Fifteenth Meeting of the International Health Regulations (2005) Emergency Committee Regarding the Coronavirus Disease (COVID-19) Pandemic. World Health Organization. https://www.who.int/news/item/05-05-2023-statement-on-the-fifteenth-meeting-of-the-international-health-regulations-(2005)-emergency-committee-regarding-the-coronavirus-disease-(covid-19)-pandemic

[4] Liu, Y., Gayle, A.A., Wilder-Smith, A. and Rocklöv, J. (2020) The Reproductive Number of COVID-19 Is Higher Compared to SARS Coronavirus. *Journal of Travel Medicine*, **27**, taaa021. https://doi.org/10.1093/jtm/taaa021

[5] Chen, C., Zhang, X., Ju, Z. and He, W. (2020) Advances in the Research of Mechanism and Related Immunotherapy on the Cytokine Storm Induced by Coronavirus Disease 2019. *Chinese Journal of Burns*, **36**, 471-475.

[6] Li, Q., Wu, J., Nie, J., Zhang, L., Hao, H., Liu, S., *et al.* (2020) The Impact of Mutations in SARS-CoV-2 Spike on Viral Infectivity and Antigenicity. *Cell*, **182**, 1284-1294.e9. https://doi.org/10.1016/j.cell.2020.07.012

[7] Wrapp, D., Wang, N., Corbett, K.S., Goldsmith, J.A., Hsieh, C., Abiona, O., *et al.* (2020) Cryo-EM Structure of the 2019-Ncov Spike in the Prefusion Conformation. *Science*, **367**, 1260-1263. https://doi.org/10.1126/science.abb2507

[8] Jackson, C.B., Farzan, M., Chen, B. and Choe, H. (2022) Mechanisms of SARS-CoV-2 Entry into Cells. *Nature Reviews Molecular Cell Biology*, **23**, 3-20. https://doi.org/10.1038/s41580-021-00418-x

[9] Lan, J., Ge, J., Yu, J., Shan, S., Zhou, H., Fan, S., *et al.* (2020) Structure of the SARS-CoV-2 Spike Receptor-Binding Domain Bound to the ACE2 Receptor. *Nature*, **581**, 215-220. https://doi.org/10.1038/s41586-020-2180-5

[10] Amin, M., Sorour, M.K. and Kasry, A. (2020) Comparing the Binding Interactions in the Receptor Binding Domains of SARS-CoV-2 and SARS-CoV. *The Journal of Physical Chemistry Letters*, **11**, 4897-4900. https://doi.org/10.1021/acs.jpclett.0c01064

[11] Yi, C., Sun, X., Ye, J., Ding, L., Liu, M., Yang, Z., *et al.* (2020) Key Residues of the Receptor Binding Motif in the Spike Protein of SARS-CoV-2 That Interact with ACE2 and Neutralizing Antibodies. *Cellular & Molecular Immunology*, **17**, 621-630. https://doi.org/10.1038/s41423-020-0458-z

[12] Di Paola, L., Hadi-Alijanvand, H., Song, X., Hu, G. and Giuliani, A. (2020) The Discovery of a Putative Allosteric Site in the SARS-CoV-2 Spike Protein Using an Integrated Structural/Dynamic Approach. *Journal of Proteome Research*, **19**, 4576-4586. https://doi.org/10.1021/acs.jproteome.0c00273

[13] Greaney, A.J., Starr, T.N., Gilchuk, P., Zost, S.J., Binshtein, E., Loes, A.N., *et al.* (2021) Complete Mapping of Mutations to the SARS-CoV-2 Spike Receptor-Binding Domain That Escape Antibody Recognition. *Cell Host & Microbe*, **29**, 44-57.e9. https://doi.org/10.1016/j.chom.2020.11.007

[14] Walls, A.C., Park, Y., Tortorici, M.A., Wall, A., McGuire, A.T. and Veesler, D. (2020) Structure, Function, and Antigenicity of the SARS-CoV-2 Spike Glycoprotein. *Cell*, **181**, 281-292.e6. https://doi.org/10.1016/j.cell.2020.02.058

[15] Gangavarapu, K., Latif, A.A., Mullen, J.L., Alkuzweny, M., Hufbauer, E., Tsueng, G., *et al.* (2023) Outbreak.Info Genomic Reports: Scalable and Dynamic Surveillance of SARS-CoV-2 Variants and Mutations. *Nature Methods*, **20**, 512-522. https://doi.org/10.1038/s41592-023-01769-3

[16] Chen, C., Nadeau, S., Yared, M., Voinov, P., Xie, N., Roemer, C., *et al.* (2021) Cov-

spectrum: Analysis of Globally Shared SARS-CoV-2 Data to Identify and Characterize New Variants. *Bioinformatics*, **38**, 1735-1737. https://doi.org/10.1093/bioinformatics/btab856

[17] Bangaru, S., Ozorowski, G., Turner, H.L., Antanasijevic, A., Huang, D., Wang, X., *et al.* (2020) Structural Analysis of Full-Length SARS-CoV-2 Spike Protein from an Advanced Vaccine Candidate. *Science*, **370**, 1089-1094. https://doi.org/10.1126/science.abe1502

[18] Pražnikar, J., Tomić, M. and Turk, D. (2019) Validation and Quality Assessment of Macromolecular Structures Using Complex Network Analysis. *Scientific Reports*, **9**, Article No. 1678. https://doi.org/10.1038/s41598-019-38658-9

[19] da Silveira, C.H., Pires, D.E.V., Minardi, R.C., Ribeiro, C., Veloso, C.J.M., Lopes, J.C.D., *et al.* (2008) Protein Cutoff Scanning: A Comparative Analysis of Cutoff Dependent and Cutoff Free Methods for Prospecting Contacts in Proteins. *Proteins*: *Structure*, *Function*, *and Bioinformatics*, **74**, 727-743. https://doi.org/10.1002/prot.22187

[20] Shannon, P., Markiel, A., Ozier, O., Baliga, N.S., Wang, J.T., Ramage, D., *et al.* (2003) Cytoscape: A Software Environment for Integrated Models of Biomolecular Interaction Networks. *Genome Research*, **13**, 2498-2504. https://doi.org/10.1101/gr.1239303

[21] Gadiyaram, V., Vishveshwara, S. and Vishveshwara, S. (2019) From Quantum Chemistry to Networks in Biology: A Graph Spectral Approach to Protein Structure Analyses. *Journal of Chemical Information and Modeling*, **59**, 1715-1727. https://doi.org/10.1021/acs.jcim.9b00002

[22] Giuliani, A., Krishnan, A., Zbilut, J. and Tomita, M. (2008) Proteins as Networks: Usefulness of Graph Theory in Protein Science. *Current Protein & Peptide Science*, **9**, 28-38. https://doi.org/10.2174/138920308783565705

[23] Hadfield, J., Megill, C., Bell, S.M., Huddleston, J., Potter, B., Callender, C., Sagulenko, P., Bedford, T. and Neher, R.A. (2018) Nextstrain: Real-Time Tracking of Pathogen Evolution. *Bioinformatics*, **34**, 4121-4123. https://doi.org/10.1093/bioinformatics/bty407

[24] Hulo, C., de Castro, E., Masson, P., Bougueleret, L., Bairoch, A., Xenarios, I. and Le Mercier, P. (2026) ViralZone: A Knowledge Resource to Understand Virus Diversity. SARS-CoV-2. https://viralzone.expasy.org/872

[25] Yang, Z., Han, Y., Ding, S., Shi, W., Zhou, T., Finzi, A., *et al.* (2022) SARS-CoV-2 Variants Increase Kinetic Stability of Open Spike Conformations as an Evolutionary Strategy. *mBio*, **13**, e03227-21. https://doi.org/10.1128/mbio.03227-21

[26] Negre, C.F.A., Morzan, U.N., Hendrickson, H.P., Pal, R., Lisi, G.P., Loria, J.P., *et al.* (2018) Eigenvector Centrality for Characterization of Protein Allosteric Pathways. *Proceedings of the National Academy of Sciences*, **115**, E12201-E12208. https://doi.org/10.1073/pnas.1810452115

[27] Borah, C. (2024) Centrality Based Analysis of Amino Acids Network. *Network Biology*, **14**, 156-173.

[28] Guzzi, P.H., di Paola, L., Puccio, B., Lomoio, U., Giuliani, A. and Veltri, P. (2023) Computational Analysis of the Sequence-Structure Relation in SARS-CoV-2 Spike Protein Using Protein Contact Networks. *Scientific Reports*, **13**, Article No. 2837. https://doi.org/10.1038/s41598-023-30052-w

[29] Cai, Y., Zhang, J., Xiao, T., Peng, H., Sterling, S.M., Walsh, R.M., *et al.* (2020) Distinct Conformational States of SARS-CoV-2 Spike Protein. *Science*, **369**, 1586-1592. https://doi.org/10.1126/science.abd4251

[30] Liu, Y., Liu, J., Johnson, B.A., Xia, H., Ku, Z., Schindewolf, C., *et al.* (2022) Delta Spike

P681R Mutation Enhances SARS-CoV-2 Fitness over Alpha Variant. *Cell Reports*, **39**, Article 110829. https://doi.org/10.1016/j.celrep.2022.110829

[31] Ozono, S., Zhang, Y., Ode, H., Sano, K., Tan, T.S., Imai, K., *et al.* (2021) SARS-CoV-2 D614G Spike Mutation Increases Entry Efficiency with Enhanced Ace2-Binding Affinity. *Nature Communications*, **12**, Article No. 848. https://doi.org/10.1038/s41467-021-21118-2

[32] He, C., He, X., Yang, J., Lei, H., Hong, W., Song, X., *et al.* (2022) Spike Protein of SARS-CoV-2 Omicron (B.1.1.529) Variant Has a Reduced Ability to Induce the Immune Response. *Signal Transduction and Targeted Therapy*, **7**, Article No. 119. https://doi.org/10.1038/s41392-022-00980-6